Density, Viscosity, and Excess Properties of Aqueous Solution of 1,3-Dimethyl-2-imidazolidinone (DMI)

Alain Valtz, Frédérick de Meyer, Christophe Coquelet

Density, viscosity and excess properties of aqueous solution of 1,3-dimethyl-2-imidazolidinone (DMI)

Alain Valtz[1], Frédérick de Meyer[2,1], Christophe Coquelet[3,1,*]

1 Mines Paris PSL University, CTP-Centre of Thermodynamics of Processes, 35 Rue Saint Honoré, 77305 Fontainebleau, France.

2 TotalEnergies S.E., OneTech, Gas and Low Carbon, CO_2 and Sustainability R&D, 2 Place Jean Millier, 92078 Paris, France.

3 Université de Toulouse, IMT Mines Albi, CNRS UMR 5302, Centre Rapsodee Campus Jarlard, 81013 Albi CT Cedex 9, France.

Abstract – A complete study of thermophysical properties concerning the 1,3-dimethyl-2-imidazolidinone (DMI) + water binary system is realized. Density, speed of sound, dynamic viscosities, and refractive index measurements have been performed at atmospheric pressure, using a vibrating tube densitometer, a falling ball viscosimeter, and a refractometer for pure DMI, pure water, and for aqueous solutions of DMI, from 278.15 to 323.15 K. The thermal expansion was calculated from density data. Excess Gibbs energy of flow and the corresponding excess entropy of flow were also calculated considering dynamic viscosity and density data. Excess molar properties (volume, thermal expansion, Gibbs energy of flow and square of refractive index) were calculated and the Redlich-Kister equations were applied to correlate the data. The analysis of the behavior of the excess properties allows to identify the most relevant molecular interaction in mixtures rich in DMI and in mixtures rich in water. Our results show that DMI can be classified as a liquid structure maker and that molecules of water are certainly inserted in the DMI network at finite dilution.

*: Corresponding author, Email: Christophe.coquelet@mines-albi.fr

1. Introduction

The knowledge of thermophysical properties of solvents is essential for the optimization or design of new efficient operation units. Solvents are used in liquid-liquid extraction processes or gas absorption processes. For example, in the context of gas processing and particularly for acid gas removal using a gas-liquid absorption column, the choice of the solvent is an essential step. These solvents are mainly composed of water and an alkanolamine like MDEA (methyldiethanolamine), DEA (diethanolamine) or MEA (monoethanolamine). Because natural gas contains several species: methane, other hydrocarbons, CO_2, H_2S, mercaptans and, to respect the specification in terms of composition for liquefied natural gas (LNG) or gas circulating in pipeline, a co-solvent can be added to improve the gas treatment. A similar comment can be formulated in the context of utilization of supercritical fluids such as supercritical water, as solvent for extraction or purification of high value molecules. The co-solvent can also be added to change the thermophysical properties of the solvent and modify the selectivity. Consequently, it is important to know and understand how the co-solvent will alter the thermophysical properties such as density, viscosity, solubility of non-reactive species, and so on.

In this paper, we have studied the densities, speed of sound, viscosities and refractive index of mixtures composed of water and one potential co-solvent. The co-solvent considered in this study is the cyclic amide 1,3-dimethyl-2-imidazolidinone (DMI). DMI is a very stable aprotic solvent with a high dipole moment (μ=4.09 D, a high dielectric constant (=37.6) and an excellent ability to solvate inorganic and organic compounds[1]. DMI is very polar and thus completely miscible with water. DMI is widely used in the manufacture of polymers, medicines, dyestuffs, agrochemicals, electronic parts, and so on. It is often utilized as a substitute for the carcinogenic hexamethylphosphoramide (HMPA).

Excess properties are also very useful to understand the mixing state in terms of intermolecular interactions. Indeed, the information concerning molecular interactions is required for the design of solvents for industrial applications. In our case, the examination of excess properties will be helpful to better understand the molecular interaction of water with the -CON-R group in DMI.

First, new experimental measurements of density and excess volume for the binary mixture composed of water and DMI are presented. Then, these new experimental excess volumes are correlated by the Redlich-Kister equation[2]. Also, the same type of correlation will be used to correlate excess dynamic viscosity and refractive index data.

2. Experimental details

2.1. Materials purities and suppliers

Table 1 presents the chemical species, suppliers, purity and refractive index. Compositions are prepared gravimetrically. Water was purified by a Millipore Direct-Q5UV system with a 0.22 μm membrane.

Table 1: Chemical sample

Compound	*CAS Number*	*Formula*	*Supplier*	*Purity (GC)*[a]	*Refractive index* (293.15 K)*	*nD*[c]
Water	7732-18-5	H_2O	-	-	1.33299	1.3325
1,3-dimethyl-2-imidazolidinone (DMI)	80-73-9	$C_5H_{10}N_20$	Sigma Aldrich	0.995	1.47259[b]	1.4704

*: Apparatus; Anton Paar ABBEMAT 300 (λ=589nm), supplier accuracy +/- 0.0001, u(n)=6 ×10^{-5}, [a]GC: Gas Chromatograph, (b): 1.472 at 20°C at λ=589nm given by the supplier (c): Value from Simulis Thermodynamics (Prosim, France): Bloxham et al.[3]

2.2. Experimental method

-Density

Density measurements have all been performed with the DSA5000M Anton Paar digital vibrating tube densimeter. The oscillating period or frequency, measured by the densitometer, is depending on the tube mass and therefore on the fluid density. Eq. 1 is used for relating the period of vibration, τ, to density, ρ:

$$\rho = a + b\tau^2 \quad (1)$$

where *a* and *b* are constants to be adjusted. For these purposes we have used bi-distilled and degassed water, and dry air, at 293.15 K. Supplier accuracy (*a*) on measured density is estimated lower than 0.01 kg.m^{-3}.

We have considered the recommendation given by Chirico et al.[4] concerning the estimate of relative density uncertainty ($u_r(\rho) = \xi(1 - x_s)$) with ξ the presumed difference in density between the compound and the impurity (the authors recommend ξ=0.1) and x_s the purity. Details on uncertainty calculation is given by Eq. 2. One platinum resistance thermometer with 0.01 K accuracy is used for temperature measurements. The sample densities are then measured at thermal equilibrium for various temperatures. This densitometer permits also the measurement of speed of sound with an accuracy of 0.5 m.s^{-1}.

$$u = \sqrt{\left(\frac{a}{\sqrt{3}}\right)^2 + \left(\rho \times u_r(\rho)\right)^2} \quad (2)$$

-Viscosity

The viscosity data have been obtained by an Anton Paar LOVIS 2000 ME viscometer. It is a modular instrument to be coupled with the densimeter DSA5000M. The solution sample is filled into a glass capillary (diameter of 1.59 mm) which is introduced into a temperature controlled capillary block. This block can be inclined at a variable predefined angle according to the calibration performed. We can note that the capillary had already been calibrated with appropriate standard fluids (see Reference Manual of Lovis[5]).

Briefly, the experimental method of LOVIS 2000 ME viscometer is based on the falling ball method. The principle consists of measuring the falling time of a steel ball in the capillary tube filled with the sample fluid and inclined at different angles. It automatically provides the viscosity value for the specified temperature level. The equation governing this principle (i.e. the calibration curve of the instrument) is given by Eq. 3.

$$\eta = K_1 * (\rho_K - \rho_S) * t_1 \quad (3)$$

where η is the dynamic viscosity of the sample solution in mPa.s; K_1 is the calibration constant of the measuring system; ρ_K is the ball (steel) density in g.cm^{-3}; ρ_S is the sample density in g.cm^{-3}, measured by the instrument, and t_1 is the rolling time in seconds. More details are given in Chirico et al.[4]. The estimate of viscosity uncertainty depends on the uncertainty of density. The calculation of the uncertainty is given by Eq. 4.

$$u = \sqrt{\left(\frac{u_B}{\sqrt{3}}\right)^2 + \left(\frac{s}{\sqrt{N}}\right)^2} \quad (4)$$

u_B , linked to the accuracy of the instrument, is equal to the 0.5% of the measured value for the LOVIS viscometer (given by Manual of Lovis[5]). The second term is the standard deviation (s) of the average of three different measurement cycles (we have considered 3 cycles). When just one cycle of measurements is performed, the uncertainty of the experimental data corresponds to the uncertainty of the instrument used (u_{RB}). More details concerning estimation of uncertainty are given in Supporting Information of the paper from Cremona et al.[6] Also, following the recommendation of Huber et al.[7], we have considered a relative expanded uncertainty equal to $U_r(\eta)=0.01$.

Refractive index of aqueous solution of DMI was measured by a refractometer from Anton Paar ABBEMAT 300 with an accuracy of measurement equal to +/- 0.0001. The refractive index was measured at 293.15 K. Atmospheric pressure is measured by a GE Druck DPI 142 Barometric Indicator with an uncertainty $u_p = 0.029$ kPa. Considering the natural variation of "atmospheric pressure" we can estimate the uncertainty of pressure measurement equal to $u_p = 0.3$ kPa.

- Preparation of mixture

To prepare the mixtures, an empty 20 cm^3 glass bottle is air-tight closed with a septum and then put under vacuum using a vacuum pump wherein a needle is introduced through the septum. The empty bottle is weighed, and then the less volatile component, freshly degassed, is introduced by means of a syringe. After weighing the bottle loaded with the first component, the more volatile one is added similarly and then the bottle is weighed again. All weightings are performed using an analytical balance with 10^{-4} g accuracy and hence the uncertainty is estimated to be lower than 2×10^{-5} for mole fractions.

3. Results and Discussions

3.1. Pure component properties

The density values of pure chemical measured using the DSA 5000M Anton Paar densitometer are presented as a function of temperature in Table 2. Comparison with literature was done and presented in Supporting Information and a good agreement is observed. The density data were used to calculate the thermal expansion ($\alpha = \frac{1}{v}\left(\frac{\partial v}{\partial T}\right)_p$). The molar volume data were correlated

by a second order polynomial expression in the temperature range 283.15-343.15 K ($v = aT^2 + bT + c$ where a, b and c are the parameters adjusted on experimental data). The parameters are presented in Table S3 in Supporting Information. Thermal expansion data are calculated considering the derivative with respect to temperature of molar volume correlation. Calculated values of thermal expansion are presented in Table 2. The dynamic viscosity data obtained with the LOVIS 2000 ME for DMI and water are also presented in Table 2.

Table 2: Density, thermal expansion and dynamic viscosity of pure components DMI and water studied at atmospheric pressure (p=101.33 kPa)[a]

	DMI			*Water*		
***T* / K**	ρ/ kg.m^{-3}	$\alpha \times 10^4 / K^{-1}$	η/ *mPa.s*	ρ/ kg.m^{-3}	$\alpha \times 10^4 / K^{-1}$	η/ *mPa.s*
283.15	1065	8.35	3.958	1000	1.34	1.306
288.15	1060	8.38	3.548	999	1.75	1.138
293.15	1056	8.40	3.204	998	2.15	1.002
298.15	1052	8.43	2.910	997	2.56	0.890
303.15	1047	8.45	2.659	996	2.96	0.797
308.15	1043	8.47	2.441	994	3.36	0.719
313.15	1038	8.50	2.252	992	3.76	0.653
318.15	1034	8.52	2.085	990	4.15	0.596
323.15	1029	8.54	1.939	988	4.55	0.547
328.15	1025	8.56	1.809	986	4.94	0.504
333.15	1021	8.58	1.695	983	5.33	0.466
338.15	1016	8.60	1.594	981	5.71	0.433
343.15	1012	8.62	1.577	978	6.09	0.404

[a]Expanded uncertainties (k=2) U(p)=0.3 kPa, U(T)=0.01 K, U(ρ)=1.0 kg.m^{-3} U(α)=2.2 10^{-5}K^{-1}, $U_r(\eta)$=0.01.

3.2. Excess properties

Excess molar volume

The measured density of aqueous DMI solutions over the entire range of mole fractions x_1 and temperature range between (283.15 and 343.15) K are listed in Table 2. Density data were used to calculate the excess volume. The excess molar volume v^E, is calculated using Eq. 5.

$$v^E = v - x_1 v_1^* - x_2 v_2^* \tag{5}$$

where x_1 and x_2 represent mole fractions and v_1^* and v_2^* are the molar volumes of components 1 and 2, respectively. v stands for the molar volume of mixture. Using the measured density ρ, Eq. 5 can be rewritten as:

$$v^E = \left[\frac{x_1 M_1 + x_2 M_2}{\rho}\right] - \frac{x_1 M_1}{\rho_1^*} - \frac{x_2 M_2}{\rho_2^*} \tag{6}$$

where M_1 and M_2 are the molar masses ρ_1^* and ρ_2^* are the densities of components (1) and (2), respectively. ρ stands for the density of the mixture. Maximum uncertainty resulting in the calculation of v^E is estimated to be less than 0.0011 $cm^3.mol^{-1}$ using Eqs. 7-9.

$$u_{\rho m} = \sqrt{u_\rho^2 + u_x^2} \tag{7}$$

$$u_{x1} = x_1 x_2 u_m \sqrt{\frac{1}{(m_1)^2} + \frac{1}{(m_2)^2}} \tag{8}$$

$$u_{v^E} = \sqrt{\left(\left(\frac{x_1 M_1 + x_2 M_2}{\rho_m^2}\right)^2 + \left(\frac{x_1 M_1}{\rho_1^2}\right)^2 + \left(\frac{x_2 M_2}{\rho_2^2}\right)^2\right) u_{\rho m}^2 + \left(\frac{M_1 + M_2}{\rho_m} - \frac{M_1}{\rho_1} - \frac{M_2}{\rho_2}\right)^2 u_x^2} \tag{9}$$

With M_i the molar mass of component i, m_i the mass of component i, ρ_i the density of component i, ρ_m density of the mixture.

Thermal expansion

Thermal expansion coefficient data are calculated using density data measured for different composition and temperature. A second order polynomial expression for the molar volume for each composition is considered (parameters are given in Table S3 in Supporting Information). Considering the definition of thermal expansion and the derivative of molar volume equation with respect to temperature for each composition, the thermal expansion was calculated. Like excess molar volume, the excess molar thermal expansion α^E, is calculated using Eq. 10.

$$\alpha^E = \alpha - x_1\alpha_1^* - x_2\alpha_2^* \quad (10)$$

where x_1 and x_2 represent mole fractions and α_1^* and α_2^* are the molar thermal expansivity of components 1 and 2 respectively. The analysis of excess thermal expansion is very important as it takes into account the influence of temperature in the variation of molar volume.

The uncertainty in thermal expansion is linked to the uncertainty in density, the accuracy of the derivative with respect to temperature, and the uncertainty in molar fraction. Eq. 11 gives the expression.

$$u_{\alpha m} = \sqrt{{u_\alpha}^2 + {u_x}^2} \quad (11)$$

The uncertainty in composition is given by Eq. 8. For the thermal expansion, uncertainty is given by Eq. 12.

$$u_\alpha = \sqrt{\left(\frac{\partial\alpha}{\partial\rho}\right)^2 u_\rho^2 + \left(\frac{\partial\alpha}{\partial T}\right)^2 u_T^2} \quad (12)$$

The value of u_α is equal to 1×10^{-5} K^{-1}. The uncertainty in excess thermal expansion is given by Eq. 13. The value obtained is also close to 1.5×10^{-5} K^{-1}.

$$u_{\alpha^E} = \sqrt{(1 + x_1^2 + x_2^2)u_\alpha^2 + (\alpha_1^2 + \alpha_2^2)u_x^2} \quad (13)$$

Refractive index

According to the theory remind by Reis et al.[8], the square of the refractive index is approximately equal to the relative permittivity ($n^2 = \varepsilon_r$). This property, also known as the dieletric constant, characterises the capability of the solvent to form electrolytes (and to stabilize

electrolytes). The refractive index is linked to the molar volume by the Lorentz-Lorenz equation (Eq. 14) as presented by Iglesias-Otero et al.[9]:

$$\left(\frac{n^2-1}{n^2+2}\right) v = \frac{N_A \alpha_p}{3\varepsilon_0} \quad (14)$$

where n is the refractive index, v the molar volume, N_A Avogadro's number, ε_0 the permittivity of vacuum and α the mean molecular polarizability. Eq. 14 was applied to estimate the excess squared refractive index $(n^2)^E$. Volume fractions instead of mole fractions are considered. Eq. 15 is considered for the calculation of excess squared refractive index.

$$(n^2)^E = n^2 - \varphi_1 n_1^2 - \varphi_2 n_2^2 \quad (15)$$

Where $\varphi_i = \frac{x_i v_i^*}{\sum_i x_i v_i^*}$ is the volume fraction of component i and n_i^2 the squared refractive index of component i.

The uncertainty in refractive index is linked to the uncertainty in refractive index measured and the uncertainty in molar fraction. Eq. 16 gives the expression.

$$u_{(n^2)m} = \sqrt{{u_{n^2}}^2 + {u_x}^2} \quad (16)$$

The uncertainty in composition is given by Eq. 8. The value of u_{n^2} is equal to 6×10^{-5}. The uncertainty in excess squared refractive index is given by Eq. 17. The value obtained is also close to 2×10^{-4}.

$$u_{(n^2)^E} = \sqrt{(1 + x_1^2 + x_2^2)u_{n^2}^2 + ((n^2)_1^2 + (n^2)_2^2)u_x^2} \quad (17)$$

Viscosity

It is more convenient to consider the kinematic viscosity instead of the dynamic viscosity. According to Eyring theory[10], kinematic viscosity can be correlated using an Arrhenius type law. An energy of activation of the flow is considered. This energy is required to activate the flow or to produce a hole of requisite size for the translation to occur. The kinematic viscosity is linked to the dynamic viscosity by Eq. 18.

$$\eta v = h N_A e^{\left(\frac{-\Delta G^*}{RT}\right)} \quad (18)$$

Where *h* is Planck's constant, N_A Avogadro's number, *v* molar volume, *T* the temperature and ΔG^* is the activation Gibbs free energy of flow. This energy can be written as the sum of contributions from the ideal solution ΔG^{*id} and the excess part ΔG^{*E}. According to Eyring, this energy is linked to excess Gibbs free energy of the mixture ΔG^E which considers the molecular interaction $\Delta G^{*E} = \sigma \Delta G^E$. The excess Gibbs free energy given by Eq. 19 is calculated from a thermodynamic model (fugacity coefficient (φ)).

$$G^E = RT \sum_{i=1}^{N} x_i \left(ln(\varphi_i^*) - ln\left(\varphi_i^0\right)\right) \quad (19)$$

Eq. 20 gives the viscosity of an ideal solution. For the real mixture, the excess Gibbs free energy of flow can be expresses by Eq. 21.

$$(\eta v)^{id} = hN_a e^{\left(\frac{-\Delta G^{*id}}{RT}\right)} \quad (20)$$

$$\Delta G^{*E} = RT\left(ln(\eta v) - x_1 ln(\eta_1 v_1) - x_2 ln(\eta v_2)\right) \quad (21)$$

3.3. Redlich-Kister data treatment

Usually the Redlich-Kister (RK) correlation[2] is chosen to correlate excess molar properties of binary systems. This equation is applied for the excess thermophysical properties. Eq. 22 presents the correlation considering mole fraction. For the refractive index, we have considered the volume fraction.

$$Y^E = x_1 x_2 \sum_i A_i (x_1 - x_2)^i \quad (22)$$

The coefficients (A_i) have to be determined. The method of calculation of the standard deviation of each parameter is given in Supporting Information file. The variance σ, corresponding to each fit, is calculated using Eq. 23.

$$\sigma = \sqrt{\left[\sum \frac{\left(Y^E - Y^E_{cal}\right)^2}{N-P}\right]} \quad (23)$$

where *P* is the number of parameters (A_n) and *N* represents the number of experimental data. The main difficulty of the RK treatment is the selection of the number of parameters A_i. In order to do that, it is recommended to investigate apparent molar properties. In our case, we have considered

$\frac{v^E}{x_1 x_2}$ as a function of molar composition x_1. This quantity gives us useful information concerning volumetric properties, particularly at low concentration as suggested by Desnoyers and Perron[11]. This term is directly related to the apparent molar volume and can thus be assimilated to a thermodynamic property. Eq. 24 shows that $\frac{v^E}{x_1 x_2}$ is directly linked to the apparent molar volume.

$$\frac{v^E}{x_1 x_2} = \frac{v_{2,\varphi} - v_2^*}{x_1} = \frac{v_{1,\varphi} - v_1^*}{x_2} \tag{24}$$

where $v_{i,\varphi}$ is the apparent molar volume. Desnoyers and Perron indicate that the change of the $\frac{v^E}{x_1 x_2}$ slope can be attributed to various factors: the first one, the size and shape of molecules, the second one, the intermolecular interaction energy differences at infinite or close to infinite dilution (in effect, at infinite dilution, $\frac{v^E}{x_1 x_2}$ decreases like the apparent molar volume) and the third one the formation of chemical complexes containing unlike molecules. There are two contributions for the apparent molar volume of a molecule: the volume of the molecule and the free volume space. By analysis of the evolution of $\frac{v^E}{x_1 x_2}$ as a function of x_1 we have selected the number of RK parameters (5) for the investigation of all excess thermophysical properties.

The partial molar volume $\overline{v_i}$ ($cm^3.mol^{-1}$) of each component *i* has been calculated using Eq. 25, with *V*, the volume of the mixture (cm^3).

$$\overline{v_i} = \left(\frac{\partial V}{\partial n_i} \right)_{T,P,n_j} \tag{25}$$

Differentiating Eq. 25 with respect to n_i and combining the result with Eq. 22 leads to equations for the partial molar volumes of the different species (Eqs. 26 and 27).

$$\overline{v_1} = v^E + v_1^* - x_2 \left(\frac{\partial v^E}{\partial x_2} \right)_{T,P} \tag{26}$$

$$\overline{v_2} = v^E + v_2^* - x_1\left(\frac{\partial v^E}{\partial x_1}\right)_{T,P} \quad (27)$$

Using the Redlich-Kister equation, we can obtain the expression of partial molar volumes (Eqs. 28 and 29) with respect to x_i.

$$\overline{v_1} = v_1^* + x_2^2 \sum A_n (1-2x_2)^n + 2x_2^2 (1-x_2) \sum n A_n (1-2x_2)^{n-1} \quad (28)$$

$$\overline{v_2} = v_2^* + (1-x_2)^2 \sum A_n (1-2x_2)^n - 2x_2 (1-x_2)^2 \sum n A_n (1-2x_2)^{n-1} \quad (29)$$

At infinite dilution Eqs 28 and 29 give Eqs. 30 and 31.

$$\overline{v_1^\infty} = v_1^* + \sum A_n (-1)^n \quad (30)$$

$$\overline{v_2^\infty} = v_2^* + \sum A_n \quad (31)$$

Concerning the uncertainty of molar volume at infinite dilution, it is given by Eq. 32.

$$u(\overline{v_i^\infty}) = \sqrt{u(v_i^*)^2 + \sum u(A_n)^2} \quad (32)$$

4. Results and discussion

4.1 Excess molar volume

Table 3 presents the values of mixture densities and excess volumes. The measured density at 293.15 and 313.15 K over the entire range of mole fractions x_1 are plotted in Figure 1. One can see that starting from x_1=0, the density increases with increasing DMI concentration, reaches a maximum value, and then decreases. The system was also studied by Uosaki et al.[12] at 298.15 and 308.15 K.

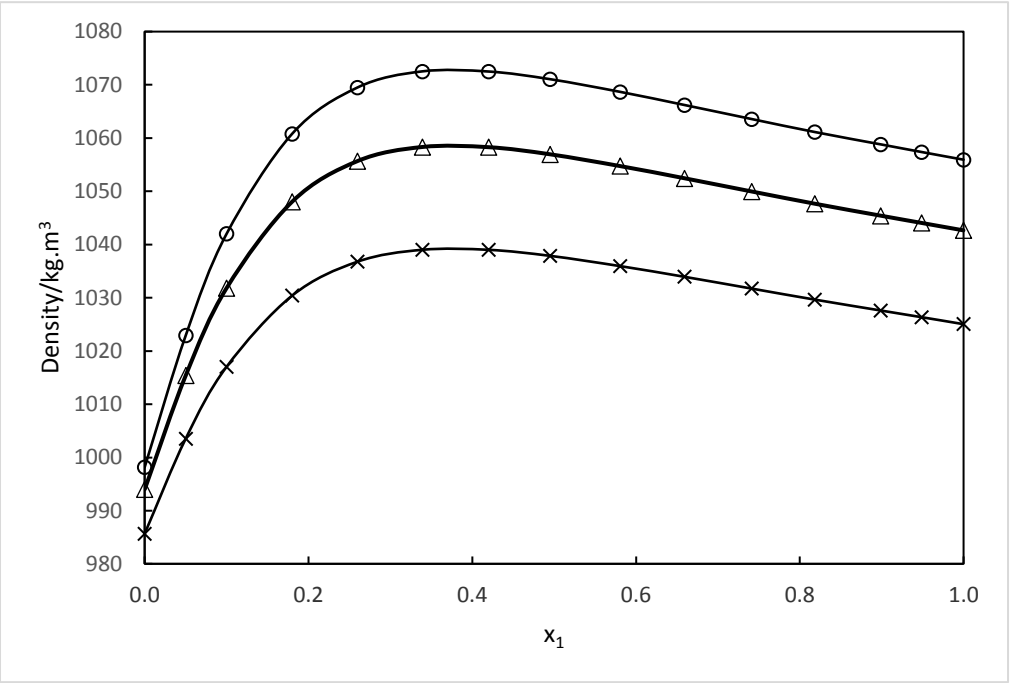

Figure 1: Density for DMI (1) + water (2) binary system as a function of DMI mole fraction at atmospheric pressure and 3 different temperatures: (○) 293.15 K, (Δ) 308.15 K, (×) 328.15 K.

Comparisons with literature data was done and presented in the Supporting Information. A good agreement is observed. Following Desnoyers and Perron's recommendations on the utilization of the Redlich Kister correlation for the data treatment, we have considered 6 Redlich Kister parameters (presented in Table 4). Figs. 2-3 present respectively, $\frac{v^E}{x_1 x_2}$ as a function of x_1 and v^E as a function of x_1, at 293.15 and 328.15 K. The excess molar volume is negative and we can observe that in absolute value, the excess volume is very important. This information supports the idea of a strong associative interaction between the two molecules. The objective of the following work is to better identify the interactions between the two molecules. The analysis of apparent molar volume does not reveal any original behavior. But we can see that for DMI close to infinite dilution, the apparent molar volume decreases, certainly due to the possible existence of a complex due to H bonds between atoms of oxygen and hydrogen of water and DMI. This complex is surrounded by molecules of water due to strong hydrophobic interactions. At the opposite, in the DMI rich region, the system under study behaves in a regular manner. Hepler[13] in 1969 has observed that it was possible to identity the effect of solute in water as structure maker or structure breaker. He indicates the partial molar heat

capacity is commonly negative in the case of structured liquid and so $\left(\partial C_P/\partial P\right)_T$ should be negative. Eq. 33 presents the thermodynamic equation that linked heat capacity and the derivative of molar volume with respect to temperature.

$$\left(\frac{\partial C_P}{\partial P}\right)_T = -T\left(\frac{\partial^2 v}{\partial T^2}\right)_P \quad (33)$$

It is possible to evaluate the effect of the solute at infinite dilution on the structure of the liquid. The temperature dependence of the molar volume at infinite dilution and the second derivative is particularly meaningful because the sign of the second derivative $\left(\frac{\partial^2 v_1^\infty}{\partial T^2}\right)_P$ can be used as one criterion to justify if DMI is a structure breaker or structure maker. In Table 5 we present the values of molar volume of DMI and water at infinite dilution as a function of temperature calculated using Redlich-Kister parameters and Eqs. 29 and 30. Considering DMI, we can correlate the molar volume at infinite dilution using a second order polynomial expression (Eq. 34).

$$v_1^\infty = 0.000215T^2 - 0.0236T + 92.91 \quad (34)$$

According to Eq. 32, we can calculate the second derivative and observed that $\left(\frac{\partial^2 v_1^\infty}{\partial T^2}\right)_P > 0$. This led to negative $\left(\frac{\partial C_P}{\partial P}\right)_T$ and so we can assume that DMI is a structure maker. It is not a surprise considering the molecular structure of DMI and the analysis of apparent or partial molar volume. In the rest of the paper, we will analyze the other thermophysical properties in order to confirm the structure maker effect of DMI with water.

Table 3: Densities (ρ /kg.m^{-3}), excess molar volumes (v^E/ cm^3.mol^{-1}), molar expansion (α / K^{-1}) and excess molar expansion (α^E /K^{-1}) for DMI *(1)* + water *(2)* binary system as a function of DMI mole fraction at atmospheric pressure (p=101.33 kPa)[a]

x_1	ρ	$\alpha \times 10^4$	v^E	$\alpha^E \times 10^4$	ρ	$\alpha \times 10^4$	v^E	$\alpha^E \times 10^4$	ρ	$\alpha \times 10^4$	v^E	$\alpha^E \times 10^4$	ρ	$\alpha \times 10^4$	v^E	$\alpha^E \times 10^4$	ρ	$\alpha \times 10^4$	v^E	$\alpha^E \times 10^4$
	T=283.15 K				T=288.15 K				T=293.15 K				T=298.15 K				T=303.15 K			
0	1000	1.34	-	-	999	1.75	-	-	998	2.15	-	-	997	2.56	-	-	996	2.96	-	-
0.0501	1027	3.87	-0.260	2.2	1025	4.16	-0.249	2.1	1023	4.45	-0.239	2.0	1021	4.74	-0.231	1.9	1018	5.03	-0.223	1.8
0.1000	1048	5.82	-0.583	3.8	1045	6.03	-0.560	3.6	1042	6.24	-0.538	3.5	1039	6.44	-0.519	3.3	1035	6.64	-0.500	3.1
0.1801	1069	7.57	-1.034	5.0	1065	7.70	-0.997	4.8	1061	7.84	-0.962	4.6	1057	7.98	-0.929	4.4	1052	8.11	-0.898	4.2
0.2598	1079	8.27	-1.328	5.1	1074	8.39	-1.286	4.9	1069	8.50	-1.246	4.7	1065	8.61	-1.208	4.5	1060	8.72	-1.170	4.3
0.3390	1082	8.52	-1.475	4.8	1077	8.62	-1.433	4.6	1073	8.72	-1.393	4.5	1068	8.82	-1.354	4.3	1063	8.92	-1.315	4.1
0.4201	1082	8.55	-1.501	4.3	1077	8.65	-1.462	4.1	1072	8.74	-1.426	4.0	1068	8.84	-1.390	3.8	1063	8.93	-1.353	3.7
0.4952	1080	8.53	-1.440	3.7	1076	8.61	-1.407	3.6	1071	8.70	-1.375	3.5	1066	8.79	-1.343	3.3	1062	8.87	-1.310	3.2
0.5807	1078	8.47	-1.299	3.1	1073	8.55	-1.272	2.9	1069	8.62	-1.247	2.8	1064	8.70	-1.220	2.7	1059	8.78	-1.193	2.6
0.6594	1075	8.41	-1.118	2.4	1071	8.48	-1.097	2.4	1066	8.55	-1.078	2.3	1062	8.61	-1.057	2.2	1057	8.68	-1.036	2.1
0.7413	1073	8.38	-0.891	1.8	1068	8.43	-0.875	1.8	1064	8.49	-0.862	1.7	1059	8.55	-0.847	1.6	1055	8.60	-0.831	1.6
0.8184	1070	8.34	-0.647	1.3	1066	8.39	-0.637	1.2	1061	8.44	-0.627	1.2	1057	8.49	-0.617	1.1	1052	8.54	-0.608	1.1
0.8990	1068	8.34	-0.377	0.7	1063	8.38	-0.371	0.7	1059	8.42	-0.368	0.6	1054	8.46	-0.362	0.6	1050	8.49	-0.357	0.6
0.9488	1066	8.34	-0.195	0.3	1062	8.37	-0.192	0.3	1057	8.40	-0.191	0.3	1053	8.43	-0.189	0.3	1048	8.46	-0.187	0.3
1	1065	8.35	-	-	1060	8.38	-	-	1056	8.40	-	-	1052	8.43	-	-	1047	8.45	-	-

[a]Expanded uncertainties (k=2) U(p)=0.3 kPa, U(T)=0.01 K, U(ρ)=1.0 kg.m^{-3} , U(x)=0.002, U(V^E)=0.011 cm^3.mol^{-1}, U(α)=2.2 10^{-5}K^{-1} , U(α^E)=4 10^{-5}K^{-1}

Table 3: Continued

x_1	ρ	$\alpha \times 10^4$	v^E	$\alpha^E \times 10^4$	ρ	$\alpha \times 10^4$	v^E	$\alpha^E \times 10^4$	ρ	$\alpha \times 10^4$	v^E	$\alpha^E \times 10^4$	ρ	$\alpha \times 10^4$	v^E	$\alpha^E \times 10^4$	ρ	$\alpha \times 10^4$	v^E	$\alpha^E \times 10^4$
	T=308.15 K				T=313.15 K				T=318.15 K				T=323.15 K				T=328.15 K			
0	994	3.36	-	-	992	3.76	-	-	990	4.15	-	-	988	4.55	-	-	986	4.94	-	-
0.0501	1015	5.31	-0.216	1.7	1013	5.59	-0.209	1.6	1010	5.87	-0.202	1.5	1007	6.15	-0.196	1.4	1004	6.42	-0.189	1.3
0.1000	1032	6.84	-0.483	3.0	1028	7.03	-0.466	2.8	1025	7.23	-0.450	2.6	1021	7.42	-0.435	2.5	1017	7.61	-0.419	2.3
0.1801	1048	8.24	-0.868	4.0	1044	8.37	-0.839	3.8	1039	8.50	-0.810	3.6	1035	8.63	-0.783	3.4	1030	8.75	-0.755	3.2
0.2598	1056	8.83	-1.134	4.1	1051	8.94	-1.099	3.9	1046	9.04	-1.063	3.8	1042	9.14	-1.029	3.6	1037	9.25	-0.994	3.4
0.3390	1058	9.02	-1.277	3.9	1054	9.12	-1.240	3.8	1049	9.21	-1.203	3.6	1044	9.31	-1.165	3.4	1039	9.40	-1.128	3.2
0.4201	1058	9.02	-1.317	3.5	1054	9.11	-1.282	3.4	1049	9.20	-1.245	3.2	1044	9.29	-1.209	3.1	1039	9.37	-1.173	2.9
0.4952	1057	8.95	-1.278	3.1	1052	9.03	-1.246	2.9	1047	9.11	-1.212	2.8	1043	9.19	-1.180	2.7	1038	9.27	-1.146	2.5
0.5807	1055	8.85	-1.166	2.5	1050	8.92	-1.138	2.4	1045	9.00	-1.110	2.3	1041	9.07	-1.082	2.2	1036	9.14	-1.052	2.1
0.6594	1052	8.75	-1.014	2.0	1048	8.81	-0.992	1.9	1043	8.88	-0.970	1.8	1039	8.94	-0.946	1.8	1034	9.00	-0.922	1.7
0.7413	1050	8.66	-0.815	1.5	1045	8.71	-0.798	1.4	1041	8.76	-0.781	1.4	1036	8.82	-0.764	1.3	1032	8.87	-0.746	1.2
0.8184	1048	8.58	-0.597	1.0	1043	8.63	-0.586	1.0	1039	8.67	-0.574	0.9	1034	8.72	-0.563	0.9	1030	8.76	-0.550	0.9
0.8990	1045	8.53	-0.350	0.6	1041	8.56	-0.344	0.5	1037	8.60	-0.338	0.5	1032	8.63	-0.332	0.5	1028	8.67	-0.325	0.5
0.9488	1044	8.49	-0.184	0.3	1040	8.52	-0.181	0.3	1035	8.55	-0.178	0.3	1031	8.58	-0.175	0.2	1026	8.61	-0.172	0.2
1	1043	8.47	-	-	1038	8.50	-	-	1034	8.52	-	-	1029	8.54	-	-	1025	8.56	-	-

[a]Expanded uncertainties (k=2) U(p)=0.3 kPa, U(T)=0.01 K, U(ρ)=1.0 kg.m^{-3} , U(x)=0.002, U(V^E)=0.011 cm^3.mol^{-1}, U(α)=2.2 10^{-5}K^{-1} , U(α^E)=4 10^{-5}K^{-1}

Table 3: Continued

x_1	ρ	$\alpha \times 10^4$	v^E	$\alpha^E \times 10^4$	ρ	$\alpha \times 10^4$	v^E	$\alpha^E \times 10^4$	ρ	$\alpha \times 10^4$	v^E	$\alpha^E \times 10^4$
		T=333.15 K				T=338.15 K				T=343.15 K		
0	983	5.33	-	-	981	5.71	-	-	978	6.09	-	-
0.0501	1000	6.69	-0.183	1.2	997	6.96	-0.176	1.1	993	7.23	-0.169	1.0
0.1000	1013	7.80	-0.404	2.1	1009	7.98	-0.389	2.0	1005	8.17	-0.374	1.8
0.1801	1026	8.88	-0.727	3.0	1021	9.00	-0.700	2.8	1017	9.12	-0.673	2.6
0.2598	1032	9.35	-0.960	3.2	1027	9.44	-0.925	3.0	1022	9.54	-0.889	2.8
0.3390	1034	9.49	-1.090	3.1	1029	9.58	-1.052	2.9	1024	9.67	-1.013	2.7
0.4201	1034	9.46	-1.135	2.8	1029	9.54	-1.097	2.6	1024	9.62	-1.058	2.5
0.4952	1033	9.35	-1.111	2.4	1028	9.42	-1.075	2.3	1023	9.50	-1.038	2.2
0.5807	1031	9.20	-1.022	2.0	1026	9.27	-0.990	1.9	1022	9.34	-0.958	1.8
0.6594	1029	9.06	-0.897	1.6	1025	9.12	-0.871	1.5	1020	9.18	-0.843	1.4
0.7413	1027	8.92	-0.727	1.2	1023	8.97	-0.707	1.1	1018	9.02	-0.685	1.0
0.8184	1025	8.80	-0.537	0.8	1021	8.84	-0.522	0.8	1016	8.89	-0.507	0.7
0.8990	1023	8.70	-0.317	0.4	1019	8.73	-0.309	0.4	1014	8.76	-0.300	0.4
0.9488	1022	8.64	-0.168	0.2	1018	8.66	-0.164	0.2	1013	8.69	-0.160	0.2
1	1021	8.58	-	-	1016	8.60	-	-	1012	8.62	-	-

[a]Expanded uncertainties (k=2) U(P)=0.3 kPa, U(T)=0.01 K, U(ρ)=1.0 kg.m^{-3} , U(x)=0.002, U(V^E)=0.011 cm^3.mol^{-1}, U(α)=2.2 10^{-5}K^{-1} , U(α^E)=4 10^{-5}K^{-1}

Table 4: Excess molar volume: Redlich-Kister parameters and deviation for DMI + water binary system.

T/K	Redlich Kister parameters												Variance σ, eq.22
	A_0	u(A_0)	A_1	u(A_1)	A_2	u(A_2)	A_3	u(A_3)	A_4	u(A_4)	A_5	u(A_5)	
283.15	-5.728	0.028	2.537	0.160	-0.807	0.320	-0.173	0.953	2.364	0.529	-2.395	1.121	0.004
288.15	-5.596	0.025	2.401	0.145	-0.701	0.291	-0.247	0.867	2.266	0.481	-2.248	1.019	0.003
293.15	-5.472	0.022	2.257	0.128	-0.594	0.257	-0.249	0.764	2.126	0.424	-2.188	0.898	0.003
298.15	-5.345	0.020	2.138	0.113	-0.507	0.227	-0.324	0.675	2.011	0.374	-2.020	0.793	0.002
303.15	-5.218	0.017	2.020	0.098	-0.433	0.198	-0.370	0.588	1.897	0.326	-1.885	0.691	0.002
308.15	-5.089	0.015	1.913	0.084	-0.379	0.170	-0.419	0.505	1.814	0.280	-1.733	0.593	0.002
313.15	-4.961	0.014	1.811	0.079	-0.317	0.158	-0.454	0.470	1.702	0.261	-1.610	0.552	0.002
318.15	-4.830	0.012	1.705	0.068	-0.268	0.137	-0.444	0.407	1.605	0.226	-1.533	0.478	0.001
323.15	-4.699	0.011	1.609	0.061	-0.222	0.123	-0.449	0.366	1.501	0.203	-1.451	0.431	0.001
328.15	-4.565	0.010	1.514	0.057	-0.180	0.114	-0.442	0.341	1.409	0.189	-1.372	0.400	0.001
333.15	-4.426	0.009	1.424	0.052	-0.166	0.104	-0.448	0.310	1.349	0.172	-1.278	0.364	0.001
338.15	-4.283	0.009	1.337	0.050	-0.142	0.100	-0.421	0.297	1.277	0.165	-1.228	0.349	0.001
343.15	-4.138	0.008	1.257	0.046	-0.112	0.092	-0.418	0.273	1.199	0.152	-1.143	0.321	0.001

Table 5: Molar volume at infinite dilution for DMI *(1)* + water *(2)* binary system.

T/ K	v_1^{∞}/ cm^3.mol^{-1}	u(v_1^{∞})/ / cm^3.mol^{-1}	v_2^{∞}/ cm^3.mol^{-1}	u(v_2^{∞})/ / cm^3.mol^{-1}
283.15	103.5	1.6	13.9	1.6
288.15	103.7	1.5	13.9	1.5
293.15	104.3	1.3	13.9	1.3
298.15	104.9	1.1	14.0	1.1
303.15	105.5	1.0	14.1	1.0
308.15	106.1	0.8	14.2	0.8
313.15	106.6	0.8	14.3	0.8
318.15	107.2	0.7	14.4	0.7
323.15	107.8	0.6	14.5	0.6
328.15	108.3	0.6	14.6	0.6
333.15	108.9	0.5	14.8	0.5
338.15	109.5	0.5	14.9	0.5
343.15	110.1	0.5	15.1	0.5

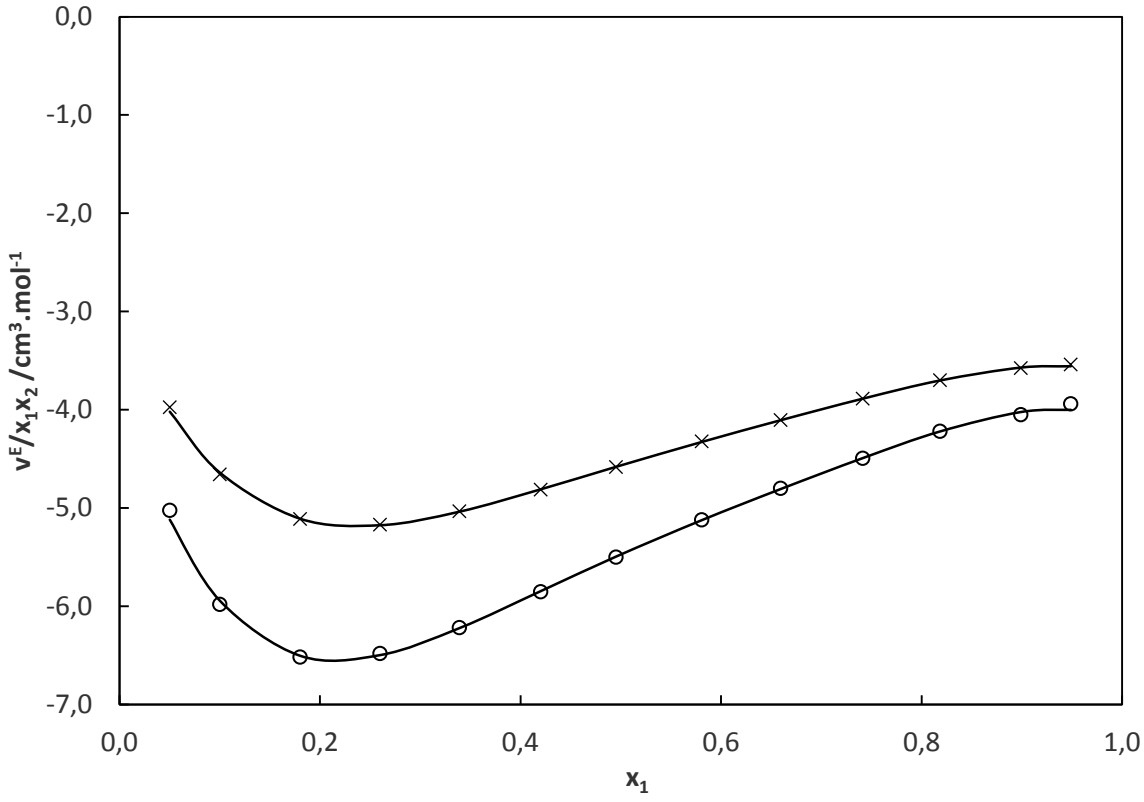

Figure 2: $\frac{v^E}{x_1 x_2}$ **for DMI (1) + water (2) system as a function of DMI mole fraction at atmospheric pressure and 2 different temperatures: (○) 293.15 K, (×) 328.15 K, solid line: Redlich-Kister correlation.**

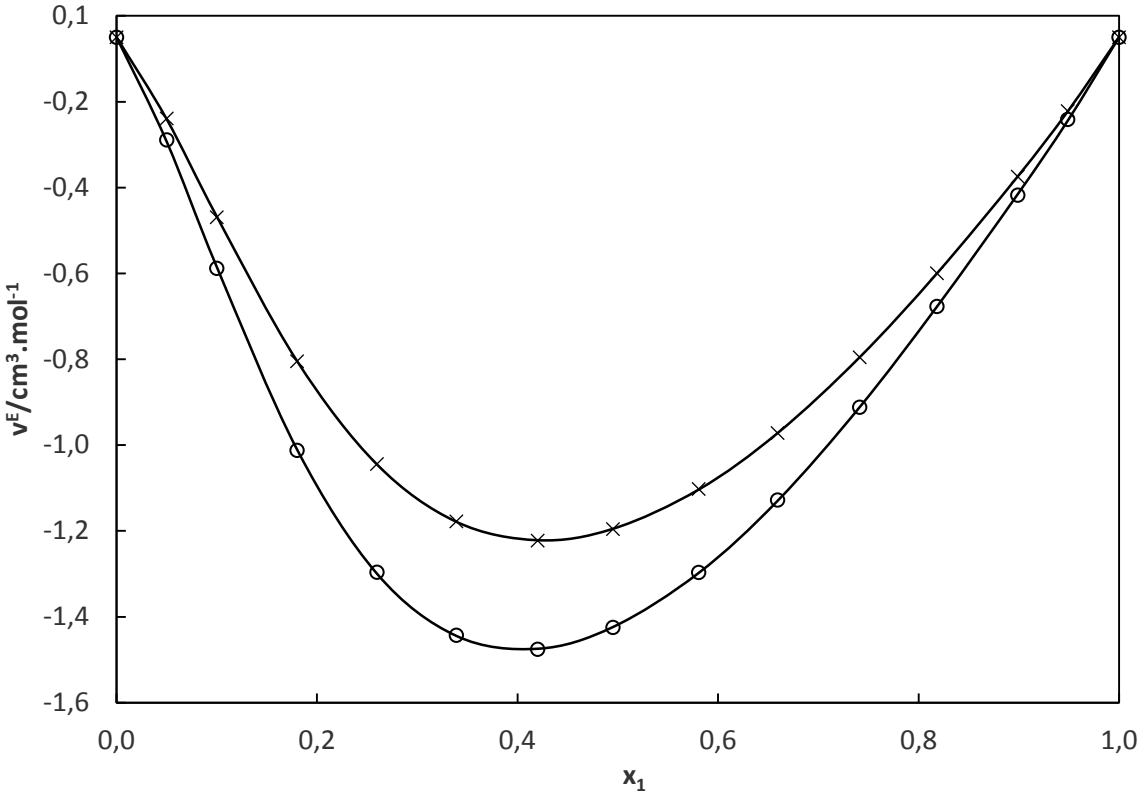

Figure 3: Excess molar volume (v^E) for DMI (1) + water (2) binary system as a function of composition at atmospheric pressure and 2 different temperatures: (○) 293.15 K, (×) 328.15 K, solid line: Redlich-Kister correlation.

4.2. Thermal expansion

The results concerning the thermal expansion are presented in Table 3. Table 6 presents the values of the Redlich-Kister parameters. We have considered the same number of parameters as for the excess volume correlation. According to Fig. 4, the excess thermal expansion shows a maximum value for a composition close to 0.2, similar to $\frac{v^E}{x_1 x_2}$. Concerning $\frac{\alpha^E}{x_1 x_2}$ (see Fig 5), there is no particular behaviour, maybe a short break in the slope of the curve. The analysis of excess thermal expansion supports the idea that there is a complex that could form for compositions close to 0.2. In order to confirm this point, we can analyse the refractive index curve at 293.15 K.

Table 6: Thermal expansion: Redlich-Kister parameters and deviation for DMI + water binary system.

T/K	Redlich Kister parameters												Variance $\sigma \times 10^6$, eq.22
	$A_0 \times 10^3$	$u(A_0) \times 10^5$	$A_1 \times 10^3$	$u(A_1) \times 10^4$	$A_2 \times 10^3$	$u(A_2) \times 10^4$	$A_3 \times 10^3$	$u(A_3) \times 10^4$	$A_4 \times 10^5$	$u(A_4) \times 10^4$	$A_5 \times 10^4$	$u(A_5) \times 10^4$	
283.15	1.462	2	-1.5	1	1.5	3	-1.4	4	3.3	9	7.1	10	3.5
288.15	1.410	2	-1.4	1	1.5	3	-1.4	8	-0.2	4	7.2	9	3.3
293.15	1.359	2	-1.4	1	1.4	3	-1.4	8	-3.5	4	7.4	9	3.2
298.15	1.308	2	-1.3	1	1.3	2	-1.3	7	-6.7	4	7.6	9	3.1
303.15	1.256	2	-1.2	1	1.3	2	-1.3	7	-9.9	4	7.8	9	3.0
308.15	1.205	2	-1.2	1	1.2	2	-1.3	7	-13.1	4	8.1	8	2.9
313.15	1.153	2	-1.1	1	1.2	2	-1.2	7	-16.2	4	8.3	8	2.9
318.15	1.102	2	-1.1	1	1.1	2	-1.2	7	-19.2	4	8.5	8	2.9
323.15	1.051	2	-1.0	1	1.0	3	-1.2	7	-22.5	4	8.7	9	3.1
328.15	1.000	2	-0.9	1	1.0	3	-1.1	8	-25.9	4	8.8	9	3.3
333.15	0.949	3	-0.9	1	0.9	3	-1.1	9	-29.4	5	9.0	10	3.6
338.15	0.898	3	-0.8	2	0.9	3	-1.1	10	-32.8	5	9.2	11	3.9
343.15	0.845	3	-0.7	2	0.8	4	-1.0	10	-36.0	6	9.3	12	4.3

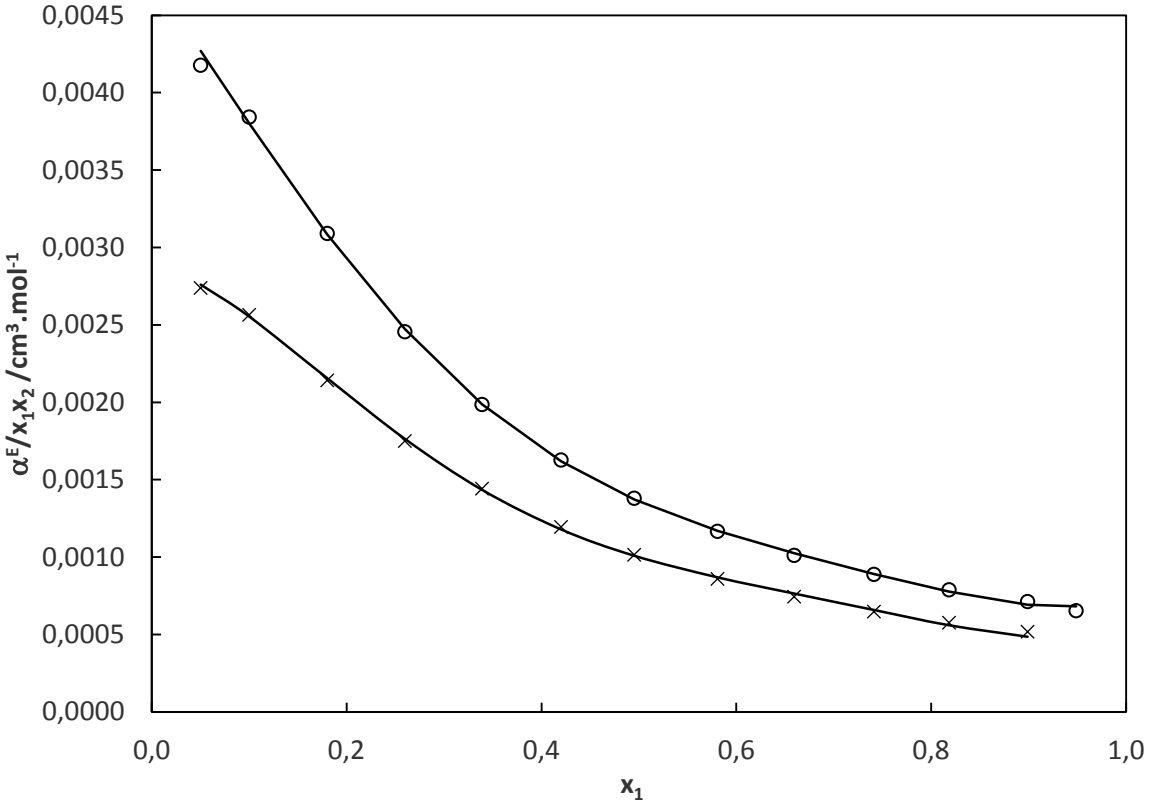

Figure 4: $\frac{\alpha^E}{x_1x_2}$ for DMI (1) + water (2) system as a function of DMI mole fraction at atmospheric pressure and 2 different temperatures: (○) 293.15 K, (×) 328.15 K, solid line: Redlich-Kister correlation.

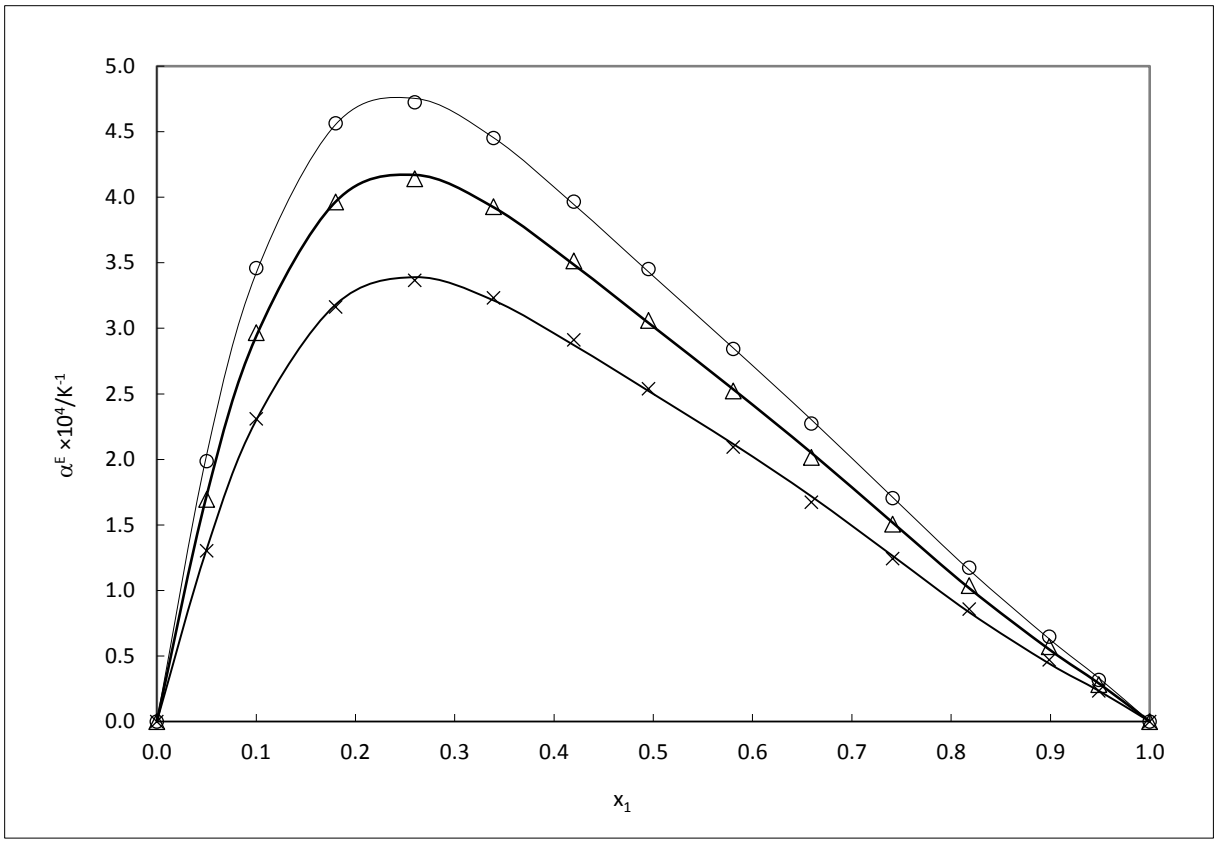

Figure 5: Excess molar expansion (α^E) for DMI (1) + water (2) binary system as a function of DMI composition at atmospheric pressure and 3 different temperatures: (○) 293.15 K, (Δ) 308.15 K, (×) 328.15 K, solid line: Redlich Kister correlation.

4.3. Refractive index

The results for the refractive index (wave length λ=589nm) at 293.15 K are presented in Table 7 and Fig. 6. No Redlich-Kister treatment was done. We can observe that the excess squared refractive index presents a maximum whereas the excess volume presents a minimum. The extrema for the two excess properties are not observed at the same composition. Iglesias-Otero et al.[9] have also demonstrated the strong link between refractive index and molar volume. Negative excess molar volume is an indication of important attractive interaction between the two molecules. The refractive index is linked to the relative permittivity also called dielectric constant. As the excess squared refractive index is always positive, we can assume that if we consider DMI + water as a solvent, the dissociating power of the solvent is increased compared to DMI and water taken alone, which is, in theory, a good characteristic for the stabilization of electrolytes. Moreover, a careful analysis of the Fig. 5 reveals a break in the curve for a composition close 0.2 in volume fraction. This can be attributed to a change in the molecular organisation maybe due to the formation of a stabilized complex composed by molecules of DMI and water.

Table 7: Refractive index and excess squared refractive index for DMI *(1)* + water *(2)* binary system as a function of DMI mole fraction at atmospheric pressure and 293.15 K (p=101.33 kPa)[a]

			volume fraction	
x_1	n	$v/\ cm^3.mol^{-1}$	φ_1	$(n^2)^E$
0.0501	1.36981	22.32	0.240	0.0055
0.1000	1.39567	26.52	0.400	0.0145
0.1801	1.42292	33.30	0.568	0.0253
0.2598	1.43962	40.20	0.678	0.0302
0.3390	1.45023	47.18	0.754	0.0308
0.4201	1.45725	54.45	0.813	0.0284
0.4952	1.46176	61.27	0.855	0.0252
0.5807	1.46531	69.10	0.892	0.0208
0.6594	1.46764	76.35	0.921	0.0165
0.7413	1.4694	83.94	0.945	0.0122
0.8184	1.47065	91.12	0.964	0.0083
0.8990	1.47163	98.64	0.982	0.0044
0.9488	1.47213	103.30	0.991	0.0021

[a]Expanded uncertainties (k=2) U(P)=0.3 kPa, U(T)=0.01 K, U(x)=0.002, $u((n^2)^E)$ =0.0002, u(n)=6 ×10^{-5}

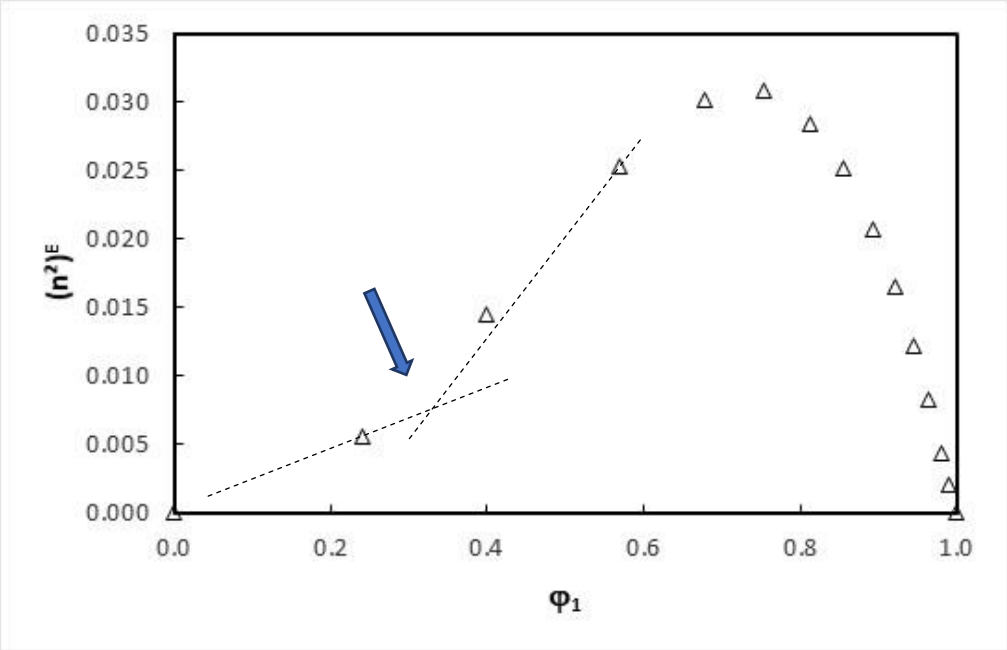

Figure 6: Excess squared refractive index for DMI (1) + water (2) binary system as a function of DMI volume fraction at atmospheric pressure and 293.15 K.

4.4. Viscosity

We have considered the kinematic viscosity for the data treatment. The results are indicated in Table 8. The kinematic viscosities increase with increasing DMI concentration and reach a maximum at composition close to 0.4 and then decrease. Using eqs. 17 to 20, we have considered excess Gibbs free energy of flow and correlated it with the Redlich-Kister equation. The Redlich-Kister parameters for the determination of excess activation Gibbs free energy are presented in Table 9. Figure 7 shows the excess Gibbs free energy of flow for DMI (1) + water (2) binary system over the whole range of compositions and at 293.15 and 318.15 K. Also, we can observe an increase of the excess Gibbs free energy of flow with increasing concentration. The maximum is reached at a concentration close to 0.3 and is followed by a decrease. We can also observe that an increasing temperature decreases the excess Gibbs free energy of flow. The concentration of the maximum remains constant. The reason of this maximum can be attributed to the apparition of a complex with strong molecular interaction between water and DMI molecules. In effect, according the Eyring theory, the excess Gibbs free energy of flow is linked to the excess Gibbs free energy calculated with the activity coefficient. When a stable complex is formed, difficulty to flow might appear, and more energy is required to move the molecules by breaking the molecular interaction. As we have performed the measurement at several temperatures, it is possible to calculate the excess entropy of flow (ΔS^{*E}) considering Eq. 35.

$$\Delta S^{*E} = -\left(\frac{\partial \Delta G^{*E}}{\partial T}\right)_P \quad (35)$$

Using our data, we have plotted on Fig. 8 the excess entropy of flow for the DMI (1) + water (2) binary system over the whole range of concentrations. The trend is the same as excess Gibbs free

energy of flow. It confirms the fact that molecular interactions between DMI are very strong especially at the composition of the maximum where it is now obvious that a complex is formed between the two molecules.

Table 8: Dynamic viscosity and excess Gibbs free energy of flow (ΔG^{*E}) for DMI *(1)* + water *(2)* binary system as a function of DMI mole fraction at atmospheric pressure (p=101.33 kPa)[a]

x_1	η /mPa.s	ΔG^{*E}/J.mol^{-1}	η /mPa.s	ΔG^{*E}/J.mol^{-1}	η /mPa.s	ΔG^{*E}/J.mol^{-1}	η /mPa.s	ΔG^{*E}/J.mol^{-1}	η /mPa.s	ΔG^{*E}/J.mol^{-1}
	T=283.15 K		T=288.15 K		T=293.15 K		T=298.15 K		T=303.15 K	
0.0501	4.413	3.019	3.697	2.978	3.142	2.943	2.704	2.914	2.354	2.892
0.1000	7.608	4.363	6.202	4.278	5.131	4.199	4.314	4.133	3.675	4.075
0.1801	13.042	5.619	10.267	5.469	8.254	5.337	6.762	5.223	5.621	5.119
0.2598	16.391	6.055	12.736	5.877	10.122	5.719	8.238	5.591	6.759	5.457
0.3390	16.602	5.923	12.973	5.750	10.345	5.593	8.408	5.455	6.948	5.332
0.4201	14.554	5.398	11.562	5.249	9.374	5.118	7.723	5.001	6.458	4.895
0.4952	12.137	4.737	9.836	4.618	8.127	4.517	6.805	4.425	5.771	4.341
0.5807	9.677	3.905	8.039	3.824	6.788	3.756	5.795	3.693	5.000	3.635
0.6594	7.825	3.104	6.645	3.056	5.712	3.013	4.954	2.971	4.338	2.934
0.7413	6.417	2.303	5.547	2.277	4.844	2.253	4.265	2.230	3.785	2.209
0.8184	5.439	1.582	4.767	1.570	4.217	1.560	3.755	1.549	3.369	1.539
0.8990	4.668	0.860	4.137	0.856	3.698	0.853	3.326	0.850	3.010	0.846
0.9488	4.295	0.434	3.827	0.431	3.439	0.430	3.108	0.428	2.827	0.427

[a]Expanded uncertainties (k=2) U(P)=0.3 kPa, U(T)=0.01 K, U(α)=2.2 10^{-5}K^{-1} , U(x)=0.002, U$_r$(η)=0.01., U(ΔG^E)=0.002 J.mol^{-1}

Table 8: Continued

x_1	η /mPa.s	ΔG^{*E}/J.mol^{-1}	η /mPa.s	ΔG^{*E}/J.mol^{-1}	η /mPa.s	ΔG^{*E}/J.mol^{-1}	η /mPa.s	ΔG^{*E}/J.mol^{-1}	η /mPa.s	ΔG^{*E}/J.mol^{-1}
	T=308.15 K		T= 313.15 K		T=318.15 K		T=323.15 K		T=328.15 K	
0.0501	2.068	2.871	1.831	2.852	1.636	2.841	1.472	2.833	1.336	2.835
0.1000	3.164	4.022	2.752	3.974	2.418	3.937	2.139	3.900	1.908	3.872
0.1801	4.736	5.026	4.040	4.941	3.482	4.867	3.032	4.800	2.662	4.741
0.2598	5.646	5.343	4.788	5.246	4.093	5.152	3.540	5.069	3.092	4.997
0.3390	5.823	5.221	4.939	5.119	4.237	5.028	3.673	4.947	3.214	4.875
0.4201	5.468	4.799	4.684	4.712	4.053	4.635	3.540	4.564	3.119	4.502
0.4952	4.951	4.265	4.290	4.196	3.752	4.135	3.308	4.078	2.939	4.028
0.5807	4.351	3.580	3.827	3.534	3.387	3.491	3.021	3.451	2.712	3.417
0.6594	3.830	2.900	3.407	2.869	3.052	2.842	2.750	2.817	2.489	2.792
0.7413	3.383	2.191	3.042	2.172	2.750	2.155	2.501	2.140	2.288	2.130
0.8184	3.041	1.531	2.761	1.523	2.519	1.516	2.309	1.509	2.127	1.505
0.8990	2.740	0.843	2.506	0.839	2.303	0.837	2.126	0.835	1.970	0.833
0.9488	2.585	0.427	2.374	0.424	2.191	0.425	2.031	0.425	1.888	0.424

[a]Expanded uncertainties (k=2) U(P)=0.3 kPa, U(T)=0.01 K, U(α)=2.2 10^{-5}K^{-1} , U(x)=0.002, $U_r(\eta)$=0.01., U(ΔG^E)=0.002 J.mol^{-1}

Table 8: Continued

x_1	η /mPa.s	ΔG^{*E}/J.mol^{-1}	η /mPa.s	ΔG^{*E}/J.mol^{-1}	η /mPa.s	ΔG^{*E}/J.mol^{-1}
	T=333.15 K		T=338.15 K		T=343.15 K	
0.0501	1.219	2.842	1.118	2.848	1.029	2.844
0.1000	1.714	3.850	1.548	3.828	1.409	3.800
0.1801	2.355	4.689	2.101	4.643	1.887	4.577
0.2598	2.723	4.934	2.417	4.875	2.161	4.786
0.3390	2.837	4.813	2.521	4.753	2.257	4.653
0.4201	2.768	4.445	2.474	4.393	2.225	4.286
0.4952	2.629	3.984	2.366	3.940	2.144	3.836
0.5807	2.450	3.386	2.225	3.356	2.033	3.251
0.6594	2.266	2.769	2.073	2.747	1.906	2.638
0.7413	2.103	2.121	1.940	2.109	1.797	1.997
0.8184	1.967	1.500	1.826	1.493	1.700	1.373
0.8990	1.832	0.830	1.709	0.823	1.603	0.701
0.9488	1.762	0.421	1.652	0.421	1.558	0.300

[a]Expanded uncertainties (k=2) U(P)=0.3 kPa, U(T)=0.01 K, U(α)=2.2 10^{-5}K^{-1} , U(x)=0.002, U_r(η)=0.01., U(ΔG^E)=0.002 J.mol^{-1}

Table 9: Excess Gibbs energy of flow: Redlich-Kister parameters and deviation for DMI + water binary system.

T/K	Redlich Kister parameters												Variance σ, eq.22
	A_0	u(A_0)	A_1	u(A_1)	A_2	u(A_2)	A_3	u(A_3)	A_4	u(A_4)	A_5	u(A_5)	
283.15	-5.728	0.028	2.537	0.160	-0.807	0.320	-0.173	0.953	2.364	0.529	-2.395	1.121	0.004
288.15	-5.596	0.025	2.401	0.145	-0.701	0.291	-0.247	0.867	2.266	0.481	-2.248	1.019	0.003
293.15	-5.472	0.022	2.257	0.128	-0.594	0.257	-0.249	0.764	2.126	0.424	-2.188	0.898	0.003
298.15	-5.345	0.020	2.138	0.113	-0.507	0.227	-0.324	0.675	2.011	0.374	-2.020	0.793	0.002
303.15	-5.218	0.017	2.020	0.098	-0.433	0.198	-0.370	0.588	1.897	0.326	-1.885	0.691	0.002
308.15	-5.089	0.015	1.913	0.084	-0.379	0.170	-0.419	0.505	1.814	0.280	-1.733	0.593	0.002
313.15	-4.961	0.014	1.811	0.079	-0.317	0.158	-0.454	0.470	1.702	0.261	-1.610	0.552	0.002
318.15	-4.830	0.012	1.705	0.068	-0.268	0.137	-0.444	0.407	1.605	0.226	-1.533	0.478	0.001
323.15	-4.699	0.011	1.609	0.061	-0.222	0.123	-0.449	0.366	1.501	0.203	-1.451	0.431	0.001
328.15	-4.565	0.010	1.514	0.057	-0.180	0.114	-0.442	0.341	1.409	0.189	-1.372	0.400	0.001
333.15	-4.426	0.009	1.424	0.052	-0.166	0.104	-0.448	0.310	1.349	0.172	-1.278	0.364	0.001
338.15	-4.283	0.009	1.337	0.050	-0.142	0.100	-0.421	0.297	1.277	0.165	-1.228	0.349	0.001
343.15	-4.138	0.008	1.257	0.046	-0.112	0.092	-0.418	0.273	1.199	0.152	-1.143	0.321	0.001

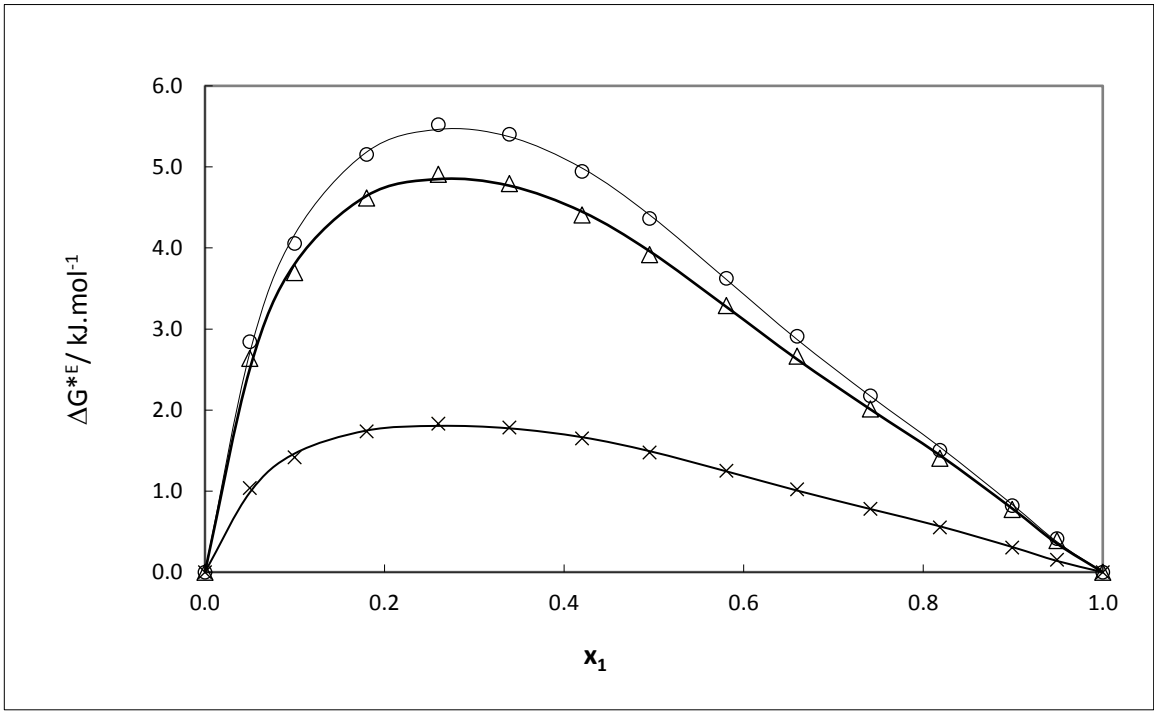

Figure 7: Excess Gibbs free energy of flow for DMI (1) + water (2) binary system as a function of DMI mole fraction at atmospheric pressure and 3 different temperatures. (○) 293.15 K, (Δ) 308.15 K , (×) 328.15 K, solid line: Redlich-Kister correlation.

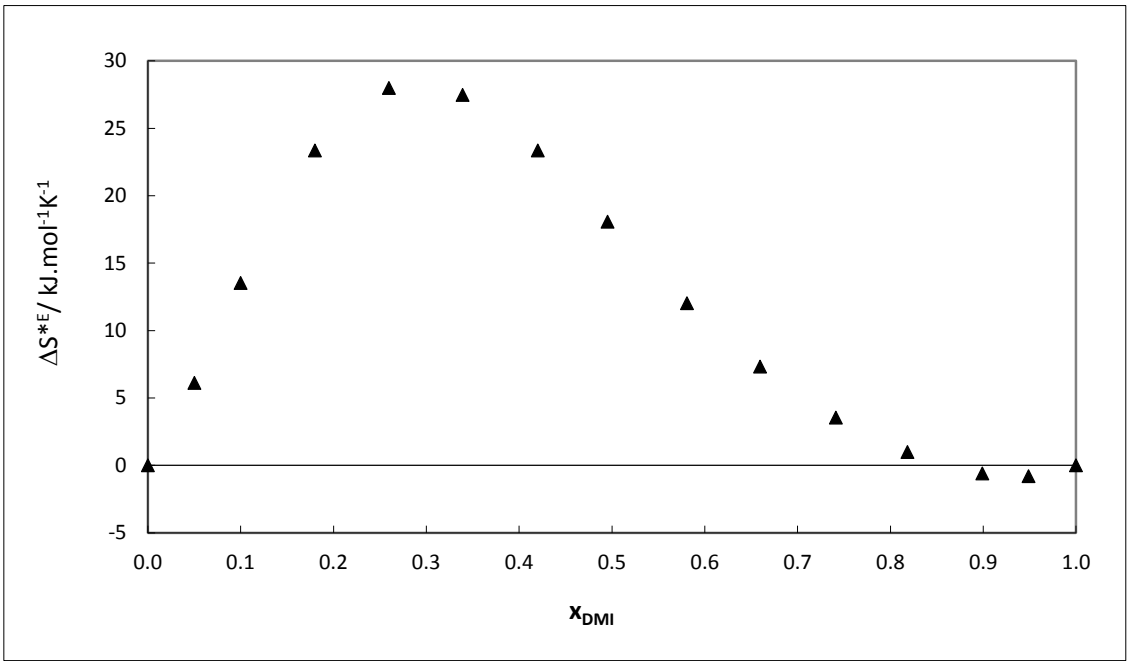

Figure 8: Excess entropy of flow for DMI (1) + water (2) binary system for whole range of mole fractions.

4.6. Discussion

Considering all our results it is now certain that a strong attractive interaction exists between the two molecules, this because the excess molar volume is negative and DMI is considered as a liquid structure maker. Probably due to the differences in size, there might be a packing effect. The analysis of apparent and partial molar volumes, refractive index, and thermal expansion reveals that there exists a composition where a complex is formed. It signifies that a stable structure exists. This stable structure is responsible for an increase of the viscosity until a concentration close to 0.2. It is important to notice that modification of the structure of the liquid appears when low quantities of DMI are introduced. An important excess of DMI destabilizes the structure of the complex. Lazarev and Mikhailov[1] have studied the structure of hydration considering FT-Raman spectroscopy measurements. In their publication, they have highlighted the phenomenon of solvation and identified a microstructure (called complex by us) stabilized by a network of intermolecular hydrogens bonds of type O-H…O, C-H…O, and N-H…O. They conclude that the cluster DMI+$(H_2O)_6$ is the optimum structure (they called it hydrate shell of monomeric molecule). According to Lazarev and Mikhailov, there is an important energy of electrostatic interactions between the charge of the cluster and the continuum of water molecules. As a consequence, it is not a surprise to observe an important excess Gibbs free energy of flow (linked to the excess Gibbs free energy). With the data we have measured, we have confirmed the existence of the cluster and also identify the composition of formation of this cluster. But we have observed the optimal cluster formation for 2 to 3 H2O molecules and 1 DMI molecule, composition slightly higher than the one identified by Lazarev and Mikhailov.

This is an important result in the case we would like to use DMI as a co-solvent in aqueous solvent (amine +water or acid + water for example): certainly, the interaction (physical or chemical) between water and the solvent might be degraded as water prefers to interact with DMI. DMI is not the only amide to present the observed behaviour. For example, Garcia-Abuin et al.[14] have studied the compressibility, the dynamic viscosity, and the excess volumes for the binary system of N-methyl-2-pyrrolidone (NMP), a cyclic amide, and water. They have observed very similar results, with a minimum excess molar volume around 40 mol% NMP. The hydrogen bonding dynamics have been studied by dielectric relaxation spectroscopy by Jia et al.[15]. They show that the size of the water clusters decreases with increasing NMP concentration. Ivanov and Kolker[16,17] have studied the binary system composed by Hexamethylphosphoramide (HMPA) and water. Heat capacity and volumetric properties were studied. They have also analysed the apparent molar properties. The profile of apparent molar volume of HMPA is very similar to DMI (the minimum is obtained for composition close to high dilution). They conclude that HMPA behave like a strongly hydrophobic solute. They observed in parallel an important increase in apparent molar heat capacity of HMPA and negative values of excess molar heat capacity. Also, in the HMPA rich region, the system behaves in a regular manner. The analysis of apparent heat capacity of water in the HMPA rich concentration region reveals a decrease in comparison to the heat capacity of pure water. The authors have concluded that no hydrogen bonds exist between molecules of water and that they are probably inserted in the holes between HMPA molecules. It is like a packing effect where HMPA molecules from a cage-type structure around the water molecule. The interaction between HMPA and water are stronger than the one between two molecules of water. We did not study the heat capacity of aqueous DMI but considering kinematic viscosity we have shown that the excess entropy of flow (linked to excess molar entropy) was negative close to infinite dilution of water. It is obvious that the negative excess

entropy we have observed also indicates an excess molar heat capacity. The conclusion mentioned for the molecule of water inserted/trapped in the cage of molecules of HMPA can be also formulated for the molecule of water at high dilution in solution of DMI.

One can compare the minimum excess molar volume of N-methyl-2-pyrrolidone (NMP), DMI and HMPA, respectively a mono-, di- and tri-amide. The values at 293 K are approximately -1.2, -1.4, and -1.6 cm^3mol^{-1} for NMP, DMI, and HMPA, respectively. Their respective dipole moments at 293 K are μ=4.1 D for NMP, μ=4.09 D for DMI and μ=5.54 D for HMPA. In the presence of water this dipole moment changes, but the very high dipole moment of HMPA likely contributes to the stronger hydrogen-bond network and thus the stronger structuring effect of HMPA. The higher minimum for the excess volume as well as the shift of this minimum to a more symmetric 40 mol% for NMP (instead of 30 mol% for DMI or HMPA) also indicates a weaker structuring effect of NMP compared to DMI or HMPA.

Additional results concerning speed of sound (for each pure component and mixtures) are presented in supporting information. The obtained results seem to also confirm the particular behaviour of the DMI + water binary system.

5. Conclusion

The densities, viscosities, speed of sound and refractive index of the DMI + water binary system were measured over the temperature range T=(283.15 – 343.15 K) using various instrument (vibrating tube densitometer, falling ball viscometer and refractometer). Excess molar volume, thermal expansion and excess Gibbs free energy of flow were determined and correlated by a Redlich-Kister correlation. From the measurements, it appears that for a given molar composition close to 0.2 in DMI, a stable cluster surrounded by molecules of water may be formed. Also, after comparison with a similar study with HMPA where molar heat capacity measurements were realized, our results seem to confirm that at infinite dilution, water molecules are inserted in the holes between DMI molecules. DMI can be classified as an aqueous liquid structure maker. It highlights the strong attractive interaction between DMI and water and thus the difficulties of using DMI as a co-solvent in an aqueous solvent. Our study shows that in order to highlight the existence of complex molecular interactions, it is preferable to have different data related to the thermodynamic properties. Density measurements combined with refractive index measurements can be used to determine excess volumes, thermal expansion, apparent molar volumes and to identify complex molecular interactions between compounds in the whole range of concentration. Kinematic viscosity measurements combined with heat capacity measurements, if available, can also provide information on the existence of these complexes. All these molecular phenomena make the prediction of solvent properties and the screening of these solvents for various gas treatment or liquid applications related to effluent treatment and purification very complicated.

Supporting information Available:

It presents comparison with literature data, the correlation used to calculate the molar volumes, the results concerning the speed of sound measurements and the method used to calculate the standard deviation of the Redlich-Kister parameters correlation.

References

[1] Lazarev, V. V.; Mikhailov, G.P. Structure of hydration shell of 1,3-dimethyl-2-imidazolidinone according to FT – Raman spectroscopy *Russ. Chem. Bul. Int. Ed.* **2015,** *64*, 1877-1881.

[2] Redlich, O.; Kister, A. Algebraic Representation of Thermodynamic Properties and the Classification of Solutions *Ind. Eng. Chem.* **1948**, *40*, 345–348.

[3] Bloxham, J. C.; Redd, M. E.; Giles, N. F.; Knotts IV, T. A.; Wilding, W. V. Proper use of the DIPPR 801 database for creation of models, methods, and processes. *J. Chem. Eng. Data* **2020**, 66, 3-10.

[4] Chirico, R. D.; Frenkel, M.; Magee, J. W.; Diky, V.; Muzny, C. D.; Kazakov, A. F.; ... & Wu, J. Improvement of quality in publication of experimental thermophysical property data: Challenges, assessment tools, global implementation, and online support. *J. Chem. Eng. Data* **2013,** *58*, 2699-2716.

[5] Anton Paar GmbH, “Reference Manual Lovis 2000 M/ME.”

[6] Cremona, R.; Delgado, S.; Valtz, A.; Conversano, A.; Gatti, M.; Coquelet, C. Density and Viscosity Measurements and Modeling of CO2-Loaded and Unloaded Aqueous Solutions of Potassium Lysinate *J. Chem. Eng. Data* **2021**, *66*, 4460-4475.

[7] Huber, M. L.; Perkins, R. A.; Laesecke, A.; Friend, D. G.; Sengers, J. V. New international formulation for the viscosity of H_2O *J. Phys. Chem. Ref. Data* **2009**, *38*, 101-125.

[8] Reis, J.C.R.; Lampreia, I.M.S.; Santos, A.F.S. ; Moita, M.L.C.J. ; Douhéret, G. Refractive index of liquid mixtures : theory and experiment *Chem. Phys. Chem*. **2010**, *11*, 3722-3733.

[9] Iglesis-otero, M.A.; Troncoso, J.; Carballo, E.; Romani, L. Density and refractive index in mixtures of ionic liquids and organic solvents: correlations and predictions *J. Chem. Thermodyn.* **2008**, *40*, 949-956.

[10] Eyring, H. Viscosity, plasticity, and diffusion as examples of absolute reaction rates J. Chem. Phys. **1936** *4* ,283-291.

[11] Desnoyers, J.; Perron, G. Treatment of Excess Thermodynamic Quantities for Liquid Mixtures *J. Solution Chem.* **1997**, *26*, 749–755.

[12] Uosaki, Y.; Sogo, K.; Kunimine, T.; Moriyoshi, T. Excess molar volumes of (cyclic amide + water) at 298.15 and 308.15K *J. Chem. Thermodyn.* **1990**, *22*, 257-262.

[13] Hepler, L.G. Thermal expansion and structure in water and aqueous solutions *Can. J. Chem.* **1969**, *47*, 4613-4617.

[14] Garcia-Abuin, A.; Gomez-Diaz, D.; La Rubia, M.D.; Navaza, J.M. Density, Speed of Sound, Viscosity, Refractive Index, and Excess Volume of N-Methyl-2-pyrrolidone + Ethanol (or Water or Ethanolamine) from T = (293.15 to 323.15) K J. Chem. Eng. Data 2011, 56, 646-651.

[15] Jia, G. Z.; Wang, F.; Yang, X. Q.; & Qian, J. The hydrogen bonding dynamics and cooperative interactions of NMP–water mixture studied by dielectric relaxation spectroscopy J. *Mol. Liq.* **2014**, 197, 328-333.

[16] Ivanov, E.V.; Kolker, A.M Thermodynamics of (water + hexamethylphosphoramide) mixtures: heat capacity properties in the temperature range between 283.15 K and 298.15 K at ambient pressure J. Chem. Thermodyn. **2021** 154, 106342.

[17] Ivanov, V.; Kustov, A.V. Volumetric properties of (water + hexamethylphosphoric triamide) from (288.15 K and 308.15) K *J. Chem. Thermodyn.* **2010** 42, 1087-1093.

Graphical Abstract